

Supplementary online materials for

Unsealing Subglacial Lake Vostok: Lessons and implications for future full-scale exploration

by V.Ya. Lipenkov, A.V. Turkeev, A.A. Ekaykin, I.A. Alekhina, A.N. Salamatin, N.I. Vasiliev

Arctic and Antarctic Research. 2024;70(4):477-498.

<https://doi.org/10.30758/0555-2648-2024-70-4-477-498>

Contents

Supplementary notes

1. Calculating drilling fluid pressure in the borehole based on fluid density measurements
2. Vostok ice core density and ice load pressure
3. Prediction of water and drilling fluid rise in the borehole after subglacial lake unsealing
4. Characterization of the ice core from the bottommost section of borehole 5G-2
5. Specifications of the Sigma-ART acoustic level meter

Supplementary tables

Table S1. Drilling fluid properties

Table S2. Ice density and load pressure

1. Calculating drilling fluid pressure in the borehole based on fluid density measurements

Drilling fluid sampling and density measurements

Drilling fluid sampling from a borehole is carried out using a three-section downhole sampler, which was designed by Nikolay Vasiliev (Fig. S1). As its name implies, the sampler design allows sampling from three different horizons of the hole in one round trip. In accordance with the practice adopted at Vostok, samples were usually drawn at 200 m intervals, starting from a 100 m depth.



Fig. S1. The three-section downhole drilling fluid sampler.

The density of each sample is measured with areometers at three or four different temperatures in the temperature range $-45\dots+5\text{C}$ (as a rule, the average of at least three readings at each temperature is taken). A correction for thermal contraction of areometers calibrated at $20\text{ }^{\circ}\text{C}$ (although it does not exceed 0.15 % of the readings) can be made using the formula:

$$\rho = \rho_{\text{meas.}}(1 - \beta\Delta T),$$

where $\rho_{\text{meas.}}$ is the measured density (areometer reading), $\Delta T = T_{\text{meas.}} - T_{\text{cal.}}$ is the difference between the measurement temperature and the temperature at which the areometer was calibrated ($20\text{ }^{\circ}\text{C}$), β is the thermal volume-expansion coefficient of the areometer ($\beta = 2.5 \cdot 10^{-5}\text{ }^{\circ}\text{C}^{-1}$).

The experimental linear density-temperature relationship established for each drilling fluid sample (see an example in Fig. S2) is then used to reduce its density to temperature T in the borehole at depth h from which the sample was drawn.

The temperature profile in the borehole $T(h)$ can be approximated by a polynomial of order 4, which at depths greater than 50 m deviates from the available experimental data [10, 13] by no more than 0.2 °C:

$$T(h) \approx -57.25 + 6.63 \cdot 10^{-3}h + 8.82 \cdot 10^{-7}h^2 + 8.19 \cdot 10^{-10}h^3 + 1.32 \cdot 10^{-13}h^4, \quad (S1)$$

where h is the true vertical depth expressed in metres and T is in °C.

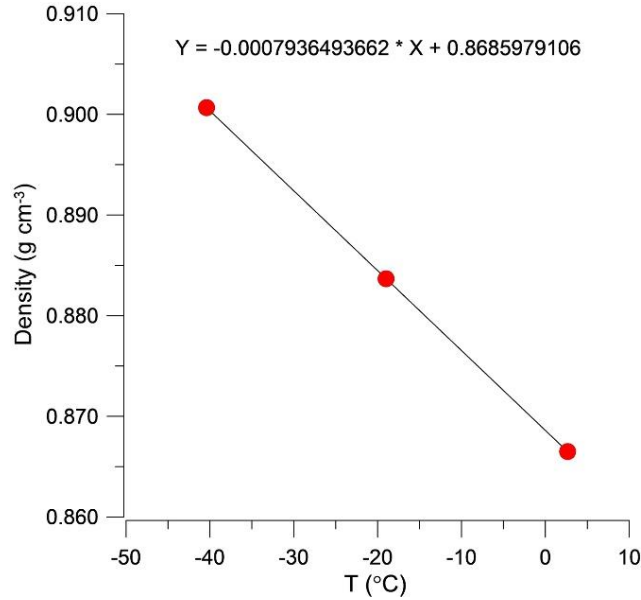


Fig. S2. Linear density-temperature relationship established for the drilling fluid sample collected from a depth of 1100 m on 12.01.2012, before the first unsealing of Lake Vostok.

When the density of the drilling fluid at a given temperature is known, the mass concentration of dichlorofluoroethane HCFC-141b in the fluid can be obtained from Table S1 ‘Drilling fluid properties’. This table has been constructed using an extensive dataset of accurate density measurements made by the hydrostatic method at various temperatures on the drilling fluid samples with different concentrations of HCFC-141b.

Alternatively, assuming that no reaction occurs between the drilling fluid components, the mass concentration of the HCFC-141b densifier, C , may be calculated from the following expression:

$$C(\%) = 100 \frac{\rho_F(\rho_f - \rho_k)}{\rho_f(\rho_F - \rho_k)}, \quad (S2)$$

where ρ_k , ρ_F and ρ_f are densities of TS-1 fuel, HCFC-141b densifier, and their mixture, respectively, at atmospheric pressure and the same temperature T ; ρ_k and ρ_F at a given temperature are calculated using experimentally established relationships:

$$\rho_k(\text{kg/m}^3) = -0.7491T(^\circ\text{C}) + 810.2 \quad (S3)$$

$$\rho_F(\text{kg/m}^3) = -1.760T(^\circ\text{C}) + 1282.7. \quad (S4)$$

Calculation of C using Eqs (S2)–(S4) reproduce the tabulated experimental data with an accuracy of at least $\pm 1\%$.

Calculation of drilling fluid pressure

The hydrostatic pressure of the drilling fluid (p_f) and the load pressure of ice (p_i) at depth h are calculated from their measured density using the same formula for rectangular integration (the midpoint rule):

$$p = g \int_0^h \rho(h) dh \approx g \sum_{j=1}^n \left[\left(\frac{\rho_{j-1} + \rho_j}{2} \right) (h_j - h_{j-1}) \right]. \quad (\text{S5})$$

Here g is the local gravity acceleration, $\rho_j = \rho(h_j)$ is the density at a discrete depth h_j ($j = 0, 1, \dots, n-1, n$).

And if the distance between data points, Δh , is constant ($\Delta h = h_n/n$), we have

$$p \approx g \Delta h \sum_{j=1}^n \left(\frac{\rho_{j-1} + \rho_j}{2} \right) \quad (\text{S6})$$

Local gravity acceleration is calculated from empirical equation [5]:

$$g \text{ (m s}^{-2}\text{)} = 9.780318 (1 + 0.005302 \sin^2 \varphi - 0.000006 \sin^2 2\varphi) - 0.000003086 E(\text{m}), \quad (\text{S7})$$

where φ is the latitude of the site, E is its altitude above sea level. For the 3769 m deep borehole drilled at Vostok (78.5°S , $E = 3488$ masl) we use $g = 9.825 \pm 0.006$ m s⁻² ($\pm 0.06\%$) calculated for $E = 1604 \pm 1884$ masl. Note that using the standard gravity acceleration (9.807 m s⁻²) instead of the local acceleration would result in an underestimation of the pressure calculated from the fluid (ice) density data by $\sim 0.2\%$.

In practice, we use the following algorithm for calculating the hydrostatic pressure of the drilling fluid from its density data.

1. The drillers' depths h_{drill} (obtained from the cable depth counter) at which the samples of the drilling fluid were drawn are converted to the true vertical depths, h , using empirical relationships presented in the main paper: $h \approx 1.0042h_{drill}$ if $h_{drill} \leq 2500$ m, and $h \approx 0.99852h_{drill} + 13.70$ when $h_{drill} > 2500$ m.
2. Measured density of the drilling fluid is reduced to the temperature in the borehole as described above.
3. Applying linear interpolation to the experimental data, a density-depth profile is obtained with the constant data spacing $\Delta h = 1$ m. (The density of the drilling fluid between the top of the fluid column and the depth at which the first fluid sample was taken is equated to the density of that sample, and the density of the fluid between the depth of the deepest sample and the hole bottom is equated to the density of that last sample.)
4. The preliminary fluid pressure distribution in the hole, $p_f^0(h)$, is then calculated, with a depth step of 1 m, using formula (S6).

5. Based on the $p_f^0(h)$ profile obtained at the previous step, calculate the drilling fluid density at temperature and hydrostatic pressure in the hole:

$$\rho_f(p_f, T) = \rho_f(T)/(1 - k_p p_f^0), \quad (S8)$$

where $\rho_f(T)$ is the fluid density at atmospheric pressure and temperature T in the hole, k_p is the fluid compressibility coefficient. For the mixture of TS-1 and HCFC-141b, we used the value of $k_p = 8 \cdot 10^{-4} \text{ MPa}^{-1}$, the validity of which was confirmed by a fairly good coincidence (within ± 0.1 MPa) of the calculated pressures with direct measurements of fluid pressure in the hole.

6. Calculate using formula (S6) the refined fluid pressure profile $p_f(h)$ based on the $\rho(p_f, T)$ data obtained at step 5. It is shown that additional iteration to further refine the values of $\rho(p_f, T)$ does not lead to a noticeable improvement and, hence, is not required.

Similarly, the finite difference method can be used to deal with the opposite task – obtaining a depth profile of the fluid density (and that of the HCFC-141b concentration) based on the results of direct measurements of fluid pressure by the downhole pressure gauge.

2. Vostok ice core density and ice load pressure

The ice core density data from [9], the calculated load pressure, p_i , and its linear approximation are given in Table S2 ‘Ice density and load pressure’. To calculate the ice load, we used Eq. (S5) and an algorithm similar to the one for the calculation of drilling fluid hydrostatic pressure. As in the case of fluid pressure, two iterations are required to obtain sufficiently accurate p_i values.

The ice density was measured only to a depth of 2540 m. At Vostok, the bubble-to-hydrate transition occurs between 500 and 1250 m [8]. Below the transition zone, the ice does not contain bubbles and its density, reduced to 0 °C and atmospheric pressure, does not change with depth and only slightly exceeds the density of pure polycrystalline ice ($916.50 \text{ kg} \cdot \text{m}^{-3}$ [1, 2]) due to the presence of air hydrates [9]. By averaging the results of density measurements in the depth range of 1300-2540 m, the maximum density of polar ice of $916.64 \pm 0.07 \text{ kg} \cdot \text{m}^{-3}$ was determined, which was then assigned to the entire ice column below 2540 m [9].

The in situ ice density was calculated based on works by T.R Butkovich [3] H. Bader [1] and A.J Gow & C. Williamson [4], in particular, a constant compressibility coefficient of $1.11 \cdot 10^{-4} \text{ MPa}^{-1}$ and a temperature-dependent thermal expansion coefficient k_T were applied:

$$k_T = - (157.556 + 0.2779T + 0.008854T^2 + 0.0001778T^3) \cdot 10^{-6}, \quad (S9)$$

where T is expressed in °C.

3. Prediction of water and drilling fluid rise in the borehole after subglacial lake unsealing

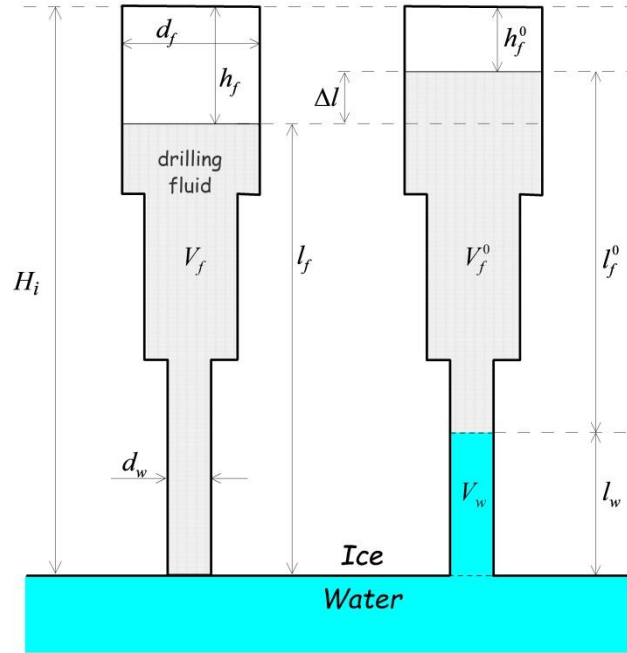


Fig. S3. Schematic of the Vostok borehole with stepwise varying diameter, showing drilling fluid and subglacial water levels just before breakthrough (left) and after pressure equalization (right).

In the figure:

H_i – the true vertical ice sheet thickness;

d_w, d_f – the borehole diameter in the bottom part of the hole and in its cased part, respectively;

l_w – the height of the water column above the lake surface;

h_f, h_f^0 – the level of drilling fluid below the casing top prior to breakthrough and after pressure equilibration, respectively;

l_f, l_f^0 – the height of drilling fluid column prior to breakthrough and after pressure equilibration;

V_w – the volume of water in the borehole ($V_w = \frac{1}{4}\pi d_w^2 l_w$);

V_f, V_f^0 – the volumes of drilling fluid in the hole prior to breakthrough and after pressure equilibration, respectively.

We define Δl and Δh_f as

$$\Delta l = l_f^0 + l_w - l_f, \quad (\text{S10})$$

$$\Delta h_f = h_f^0 - h_f - \text{the fluid-level rise in the hole following breakthrough.}$$

The increase of total volume of liquids in the hole due to water inflow is

$$V_f^0 + V_w - V_f = \frac{1}{4}\pi d_f^2 \Delta l.$$

Neglecting thermal-expansion and compressibility effects we assume: $V_f^0 = V_f$. Then

$$d_w^2 l_w = d_f^2 \Delta l, \text{ and hence}$$

$$\Delta l = l_w \frac{d_w^2}{d_f^2}. \quad (\text{S11})$$

Since $\Delta l = -\Delta h_f$, we can write Eq (3) of the main text of the paper:

$$\Delta h_f = -l_w \left(\frac{d_w}{d_f} \right)^2$$

Assuming equality between the ice overburden and the subglacial water pressure, after pressure equalization at the point of water inflow we have

$$H_i \langle \rho_i \rangle = l_w \langle \rho_w \rangle + l_f^0 \langle \rho_f \rangle, \quad (\text{S12})$$

where $\langle \rho_i \rangle$, $\langle \rho_w \rangle$, and $\langle \rho_f \rangle$ are the mean (effective) densities of ice, water, and of the drilling fluid columns, respectively, as defined in the main text, i.e.: $\langle \rho \rangle = P/gl$, where g is the local gravity acceleration; l and P are, respectively, the height of the column being considered and the hydrostatic pressure at its base.

Combining Eq.(S12) with Eqs. (S10) and (S11), we obtain

$$H_i \langle \rho_i \rangle = l_w \langle \rho_w \rangle + \langle \rho_f \rangle \left(l_f - l_w + l_w \frac{d_w^2}{d_f^2} \right).$$

Solving this equation with respect to l_w we obtain Eq. (2):

$$l_w = \left(\frac{\langle \rho_i \rangle}{\langle \rho_f \rangle} H_i - l_f \right) \left[\frac{\langle \rho_w \rangle}{\langle \rho_f \rangle} + \left(\frac{d_w}{d_f} \right)^2 - 1 \right]^{-1}.$$

Before applying Eq. (2) for predicting l_w , the value of l_f should be corrected for a small (~ 2 m) drop in the fluid level due to the fluid drained from the hole by the cable and, if applicable, for addition of kerosene in the hole during the unsealing run.

The equations (2) and (3) can be used with values of l_f , corresponding to either the case when the drill is outside the hole, or when it is at the bottom of the hole.

4. Characterization of the ice core from the bottommost section of borehole 5G-2

Thin section studies performed on a continuous basis along the 5G-1 and 5G-2 cores have provided quantitative data on the ice texture and fabric in the 230m thick stratum of accreted ice, down to the surface of Lake Vostok at a depth of 3769.3 m [7]. It was shown that the general tendency in the evolution of lake ice texture is the increase in the mean crystal size as the depth increases and the ice becomes younger towards the ice-water interface. This led to the conclusion that the main mechanism of ice accretion in Lake Vostok could be orthotropic crystal growth, similar to that which is typical for the lake ice of surface lakes.

The study revealed no presence of the fine-grained ice that would occur at the ice-water contact zone if the consolidation of loose frazil ice crystals by slow freezing of the host water was the main mechanism of lake ice formation (see, e.g., [7,11]). Instead, an enormously large monocrystal of ice, with a vertical dimension of about 3.5 m and an even bottom surface (Fig. S4) was discovered in the 5G-2 hole, at the contact with the lake water (i.e. no grain boundaries were observed in thin sections made from the lowest 3.5 metres of the core, including the broken ice core retrieved in the last drilling run in borehole 5G-2 (Fig. S5)).

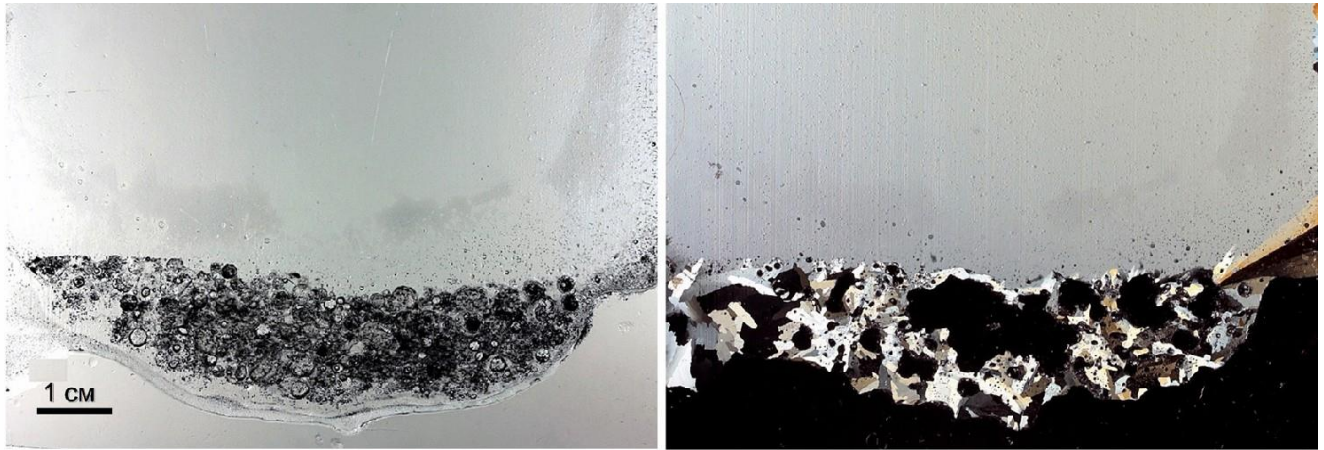


Fig. S4. A vertical thin section of the lowest part of the last 5G-2 core (see Fig. S5), photographed in plain transmitted light (left) and between crossed polarizers (right).

The photos depict the very bottom of a giant ice monocrystal found at the base of the accreted ice column, with an even surface at the ice-water interface, which is coated by a thin layer of frozen lake water that entered the borehole after the lake's unsealing.



Fig. S5. The last ice core from borehole 5G-2 recovered on February 6, 2012 after the unsealing of Lake Vostok.

The most notable feature of the last 5G-2 core is the presence on its surface of a yellowish crust, ~5 mm thick, representing frozen lake water contaminated by microscopic particles ranging in size from micrometres to several hundred micrometres (Fig. S5).

The study of the elemental compositions of more than 100 particles showed that most of them are ferrous oxides, often with an admixture of nickel, copper and zinc, i.e., elements corresponding to the composition of the core barrel [6]. It was concluded that these particles are of technogenic origin and are associated with rapid metal oxidation after the drill's contact with the lake water.

5. Specifications of the Sigma-ART acoustic level meter



Fig. S6. The Sigma-ART acoustic level meter used to measure the level of drilling fluid in the Vostok borehole.

Sigma-ART is a self-contained small-sized device (see Fig. S6) that combines the functions of acoustic wave generation, reception of transmitted and reflected signals, signal conditioning and digital indication of the level in length units with a resolution of about 1 cm. The level meter is designed for operational control of static and dynamic level in artesian wells with open access to the wellbore.

Level measurements are conducted by an operator who, standing directly above the borehole mouth, takes and records timestamped readings. Fluid level data are then synchronized with other drilling parameters independently recorded by the AMT data acquisition module (see main text).

Since the soundwave velocity strongly depends on the air properties, the instrument should be pre-tuned and calibrated for specific conditions prevailing in the hole casing at Vostok Station (low temperature, kerosene and Freon vapours).

After calibration against a float level gauge, the acoustic meter allowed us to monitor the fluid level, h_f , with an accuracy of ± 1.5 m.

References

1. Bader H. Density of ice as a function of temperature and stress: CRREL Spec. Rep. 64. 1964. 6 p.
2. Butkovich T. R. Density of single crystals of ice from a temperate glacier. J. Glaciol. 1955, 2 (18): 553–559.
3. Butkovich T.R. Linear thermal expansion of ice. US Army SIPRE Res. Rep. 40. 1957. 9 p.
4. Gow A.J., Williamson T.C. Linear compressibility of ice. J. Geophys. Res. 1972, 77 (32): 6348– 6352.

5. Grushinsky N.P. Basics of gravimetry. Moscow: Nauka. 1983. 352 p. [in Russian].
6. Leitchenkov G.L., Antonov A.V., Luneov P.I., Lipenkov V.Y. 2016 Geology and environments of subglacial Lake Vostok. Philosophical Transactions of the Royal Society A. 2016, 374: 20140302. <http://dx.doi.org/10.1098/rsta.2014.0302>
7. Lipenkov V.Y., Ekaykin A.A., Polyakova E.V., Raynaud D. Characterization of subglacial Lake Vostok as seen from physical and isotope properties of accreted ice. Philosophical Transactions of the Royal Society A. 2016, 374:20140303. <http://doi.org/10.1098/rsta.2014.0303>
8. Lipenkov V.Ya. Air bubbles and air-hydrate crystals in the Vostok ice core. In Hondoh, T. ed. Physics of ice core records. Sapporo, Hokkaido University Press. 2000, 327-358.
9. Lipenkov V.Ya., Salamatin A.N., Duval P. Bubbly-ice densification in ice sheets: II. Application. J. Glaciol. 1997, 43 (145): 397-407.
10. Lipenkov V.Ya., Turkeev A.V., Vasiliev N.I., Ekaykin A.A., Poliakova E.V. Melting temperature of ice and total gas content of water at the ice-water interface above subglacial Lake Vostok. Arctic and Antarctic Research. 2021, 67(4): 348–367. [In Russian] <https://doi.org/10.30758/0555-2648-2021-67-4-348-367>
11. Montagnat M., Duval P., Bastie P., Hamelin B, Brissaud O., de Angelis M., Petit J.R., Lipenkov V.Y. High crystalline quality of large single crystals of subglacial ice above Lake Vostok (Antarctica) revealed by hard X-ray diffraction. Sciences de la Terre et des planets. Earth Planet. Sci. 2001, 333: 419–425.
12. Souchez R., Petit J.R., Tison J.L., Jouzel J., Verbeke V. Ice formation in subglacial Lake Vostok, Central Antarctica. Earth Planet. Sci. Lett. 2000, 181: 529–538. [https://doi.org/10.1016/S0012-821X\(00\)00228-4](https://doi.org/10.1016/S0012-821X(00)00228-4)
13. Tsyganova E.A., Salamatin A.N. Non-stationary temperature field simulations along the ice flow line “Ridge B — Vostok Station”, East Antarctica. Materialy gliatsiologicheskikh issledovaniy. Data of Glaciological Studies. 2004, 97: 57–70. [In Russian]